

Constructal complex-objective optimization of electromagnet based on magnetic induction and maximum temperature difference

Shuhuan Wei, Lingen Chen*, and Fengrui Sun
Postgraduate School, Naval University of Engineering,
Wuhan 430033, P.R. China,
Fax: 0086-27-83638709, Tel: 0086-27-83615046,
*e-mail: lgchenna@yahoo.com; lingenchen@hotmail.com

Recibido el 27 de enero de 2010; aceptado el 3 de marzo de 2010

The good performance of an electromagnet requires high magnetic induction and a low temperature. A new complex-objective function reflected magnetic induction and maximum temperature difference is set up, and the electromagnet is optimized using the new complex-objective function. The optimization results show that the performance of the electromagnet is improved as the number of high thermal conductivity cooling discs inserted increases. When the performance of the electromagnet achieves its best level, the solenoid becomes longer and thinner as the number of high thermal conductivity cooling discs increases. Simultaneously, the magnetic induction becomes higher and the maximum temperature difference becomes lower. The optimized performance of the electromagnet also improves as the volume of solenoid increases; simultaneously, the magnetic induction first increases and then decreases, and the maximum temperature difference decreases all along.

Keywords: Constructal theory; electromagnet; complex-objective optimization.

El buen funcionamiento de un electroimán requiere de una alta inducción magnética y una baja temperatura. Los resultados de la optimización demuestran que el funcionamiento del electroimán mejora al incrementar el número de discos de enfriamiento de alta conductividad térmica insertados. Cuando el funcionamiento del electroimán alcanza su mejor nivel, el solenoide llega a ser más largo y más fino mientras que el número de discos de enfriamiento de alta conductividad térmica aumenta. Simultáneamente, la inducción magnética llega a ser más alta y la diferencia de la temperatura máxima disminuye. El funcionamiento optimizado del electroimán también mejora mientras que el volumen de solenoide aumenta; simultáneamente, la inducción magnética primero aumenta y después disminuye, y la diferencia de la temperatura máxima disminuye.

Descriptores: Teoría constructal; electroimán; optimización complejo-objetiva.

PACS: 057.70.-a; 01.40G

1. Introduction

Constructal theory [1-12] was generated by the study of the configuration of flow systems. The constructal law was stated as follows: For a flow system to persist in time (to survive), it must evolve in such a way that it provides easier and easier access to the current that flows through it. More and more scholars have used constructal theory to optimize the performance of heat transfer systems [13-32].

Electromagnets, which generate magnetic fields by electricity, have a wide variety of applications in domestic affairs and industry. In recent years, a most important tendency in electromagnet development is miniaturization, which means light-weight, low power dissipation and a high magnetic field. Miniaturization also brings a challenge to the electromagnet design, that is, how to prevent overheating in a compact design. It is the key point to improving the transforming efficiency between the electrical field and magnetic field while keeping the electromagnet in a steady working state. Gosselin and Bejan [33] proposed a method of optimizing the geometry of an electromagnet by maximizing its magnetic performance and thermal performance by adding

high heat transfer material to the electromagnets, using constructal theory. The electromagnets were optimized based on the minimization of the maximum temperature difference in the electromagnet for safety considerations. Chen *et al* [34] considered that the electrical resistance increases with the increase in temperature and leads to higher power dissipation, and that the mechanical strength of the solenoid decreases with the increase in the structure's temperature, and made a further multidisciplinary optimization of electromagnets on the basis of minimization of entransy dissipation rate [35]. For the heat generation in the electromagnet to increase as the magnetic induction increases, the constructal optimization based on maximum temperature difference minimization or entransy dissipation rate minimization cannot ignore the temperature increase caused by the magnetic induction increase. The optimization results in Refs. 34 and 35 are under the condition that the magnetic induction should be fixed. This paper proposes a new complex-objective function of magnetic induction and maximum temperature difference to describe the performance of electromagnets, and the configuration of electromagnets is re-optimized.

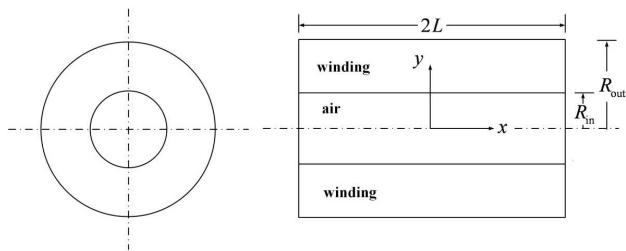


FIGURE 1. The main features of solenoid geometry [33].

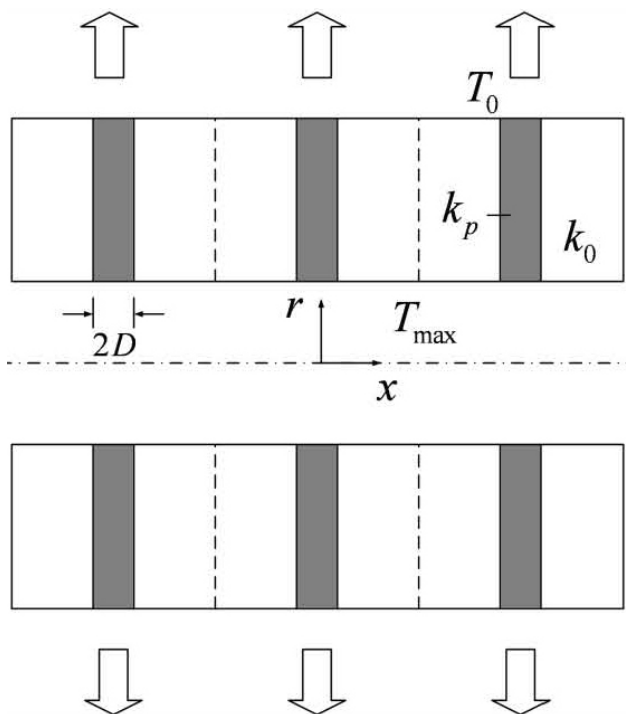


FIGURE 2. Solenoid cooled by transversal discs with high thermal conductivity [33].

2. Maximum temperature difference variation caused by electromagnet configuration

A cylindrical coil is taken as an example in this paper. Figure 1 shows the front and side views of the solenoid. A wire is wound in many layers around a cylindrical space of radius R_{in} . The outer radius of the coil is R_{out} , and the axial length is $2L$. The solenoid is considered as a continuous medium in which the electric current density j is a constant. The electrical current density inside the wire generates a one-dimensional magnetic field on the axis of symmetry of the coil. The heat generation rate per unit volume q''' is constant in the working state.

The high thermal conductivity cooling discs of thickness $2D$ are inserted into the solenoid to enhance heat transfer, and the discs are transversal and separate the solenoid into N sub-coils, as illustrated in Fig.2. The fraction of the volume occupied by the discs is known and fixed by

$$\phi = \frac{DN}{L} \tag{1}$$

where N is the number of discs. Most of the volume must be filled by the winding, as required by the drive toward compactness, therefore $\phi \ll 1$. This means that the presence of the discs does not significantly affect the magnetic field. The thermal conductivity of the material is related to its structure, density, hydrous rate, temperature, etc. But the compactness of the solenoid filled by the winding is not propitious to heat conduction; and the thermal conductivities of the wire insulating materials commonly are: polystyrene 0.08, rubber 0.202-0.29, PVC 0.17, PU 0.25, etc. The thermal conductivity of high thermal conductivity materials commonly are silver 429, copper 401, gold 401, aluminum 237, etc. The thermal conductivity of high thermal conductivity materials is defined as k_p , and the thermal conductivity of the solenoid is defined as k_0 , so that $k_0/k_p \ll 1$. It is assumed that all the boundaries are adiabatic except the exposed external surfaces of the discs, which serve as heat sinks; the heat transfer direction in the k_0 material is the x -direction, and the heat transfer direction in the k_p material is the r -direction.

The maximum temperature difference of the solenoid is [33]

$$\begin{aligned} \Delta \tilde{T} &= \frac{\Delta T}{P/(R_{in}k_0)} = \frac{\tilde{L}}{2\pi N^2 (\tilde{R}_{out}^2 - 1)} \\ &+ \frac{1}{2\pi\phi\tilde{k}\tilde{L}} \left(\frac{1}{2} - \frac{\ln \tilde{R}_{out}}{\tilde{R}_{out}^2 - 1} \right) \end{aligned} \tag{2}$$

where

$$(\tilde{R}_{out}, \tilde{L}) = \frac{(R_{out}, L)}{R_{in}}. \tag{3}$$

The solenoid is constructal optimized based on the minimization of the maximum temperature difference in Ref. 33. As shown in Fig. 3, the maximum temperature difference increases as the magnetic induction increases. The optimization results of Ref. 33 were obtained for a fixed magnetic induction.

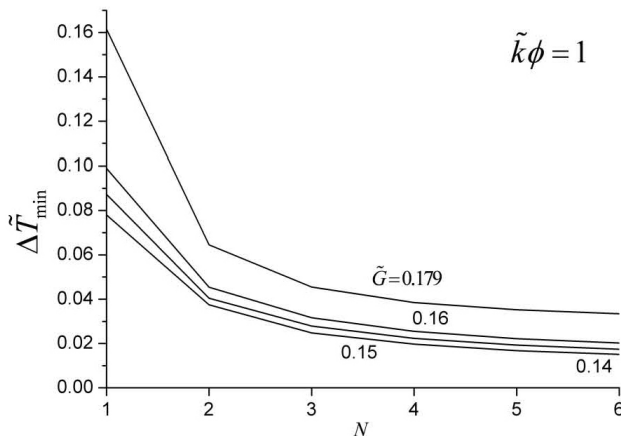


FIGURE 3. Effect of \tilde{G} on $\Delta \tilde{T}_{min}$ versus N with fixed $\tilde{k}\phi$.

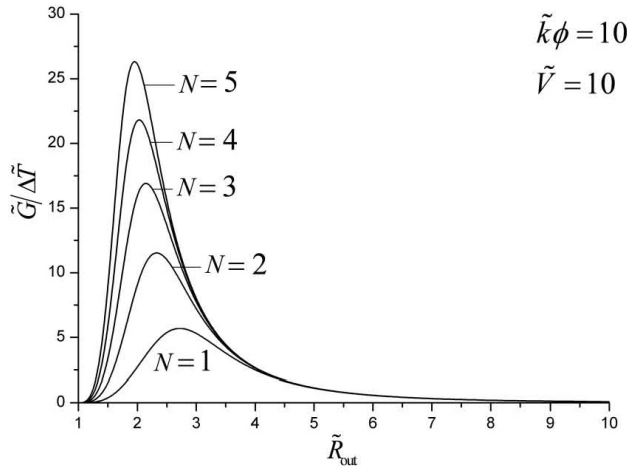


FIGURE 4. Effect of N on $\tilde{G}/\Delta\tilde{T}$ versus \tilde{R}_{out} with fixed $\tilde{k}\phi$ and \tilde{V} .

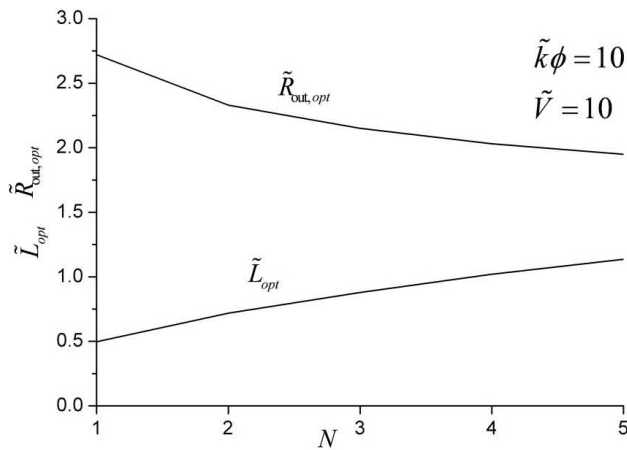


FIGURE 5. Optimal geometries $(\tilde{L}_{opt}, \tilde{R}_{out,opt})$ corresponding to $(\tilde{G}/\Delta\tilde{T})_{max}$ versus N .

3. Complex-objective function of maximum temperature difference and magnetic induction

For the case of a constant electrical current density j , the magnetic induction is given by [33]

$$\tilde{G} = 0.2 \left(\frac{2\pi\tilde{L}}{\tilde{R}_{out}^2 - 1} \right)^{1/2} \ln \frac{\tilde{R}_{out} + (\tilde{L}^2 + \tilde{R}_{out}^2)^{1/2}}{1 + (\tilde{L}^2 + 1)^{1/2}} \quad (4)$$

As Eqs. (2) and (4) show, the maximum temperature difference and magnetic induction are both related to the electromagnet configuration. A complex-objective function to describe the maximum temperature difference and magnetic induction is defined as

$$\frac{\tilde{G}}{\Delta\tilde{T}} = \frac{0.2 \left(\frac{2\pi\tilde{L}}{\tilde{R}_{out}^2 - 1} \right)^{1/2} \ln \frac{\tilde{R}_{out} + (\tilde{L}^2 + \tilde{R}_{out}^2)^{1/2}}{1 + (\tilde{L}^2 + 1)^{1/2}}}{\frac{\tilde{L}}{2\pi N^2 (\tilde{R}_{out}^2 - 1)} + \frac{1}{2\pi\phi\tilde{k}\tilde{L}} \left(\frac{1}{2} - \frac{\ln \tilde{R}_{out}}{\tilde{R}_{out}^2 - 1} \right)} \quad (5)$$

The performance of the electromagnet requires a low maximum temperature difference and high magnetic induction. Defining $\tilde{G}/\Delta\tilde{T}$ as the optimization objective can satisfy the requirement. The higher $\tilde{G}/\Delta\tilde{T}$ is, the better the performance of the electromagnet. $\tilde{G}/\Delta\tilde{T}$ is a complex-objective function that can describe the performance of the electromagnet. It is the most important improvement of this paper over Ref. 33.

A dimensionless volume is defined as [33]

$$\tilde{V} = \frac{V}{R_{in}^3} = \pi\tilde{L}(\tilde{R}_{out}^2 - 1). \quad (6)$$

Substituting Eq. (4) into Eq. (3) yields the complex-objective function combining the magnetic induction with maximum temperature difference:

$$\frac{\tilde{G}}{\Delta\tilde{T}} = \frac{\sqrt{2}}{5} \frac{\ln \left[\left[\tilde{R}_{out} + \left[\left(\frac{\tilde{V}}{\pi(\tilde{R}_{out}^2 - 1)} \right)^2 + \tilde{R}_{out}^2 \right]^{\frac{1}{2}} \right] \right]}{\frac{\tilde{V}^{1/2}}{2\pi^2 N^2 (\tilde{R}_{out}^2 - 1)} + \frac{(\tilde{R}_{out}^2 - 1)^2}{2\phi\tilde{k}\tilde{V}^{3/2}} \left(\frac{1}{2} - \frac{\ln \tilde{R}_{out}}{\tilde{R}_{out}^2 - 1} \right)}. \quad (7)$$

4. Optimization of the electromagnet

4.1. Maximization of $\tilde{G}/\Delta\tilde{T}$ at a different N

$\tilde{G}/\Delta\tilde{T}$ versus R_{out} at a different N is shown in Fig. 4. There exists an $\tilde{R}_{out,opt}$ that $\tilde{G}/\Delta\tilde{T}$ achieves its maximum and the performance of electromagnet achieves its best. The bigger N is, the bigger $(\tilde{G}/\Delta\tilde{T})_{max}$ is, and the better the performance of the electromagnet is.

$\tilde{R}_{out,opt}$ and \tilde{L}_{opt} at the maximum $\tilde{G}/\Delta\tilde{T}$ versus N characteristics are shown in Fig. 5. $\tilde{R}_{out,opt}$ decreases as N increases, and \tilde{L}_{opt} increases as N increases. When the per-

formance of the electromagnet achieves its best, the solenoid becomes longer and thinner as N increases.

When the performance of the electromagnet achieves its best, the corresponding \tilde{G} versus N and $\Delta\tilde{T}$ versus N characteristics are shown in Fig. 6 and Fig. 7, respectively. As N increases, the magnetic induction \tilde{G} increases and the maximum temperature difference $\Delta\tilde{T}$ decreases. The magnetic induction ability and heat transfer ability are both improved as N increases.

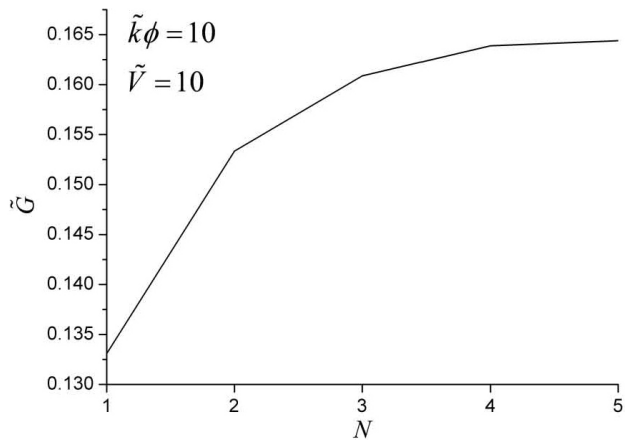


FIGURE 6. \tilde{G} corresponding to $(\tilde{G}/\Delta\tilde{T})_{\max}$ versus N .

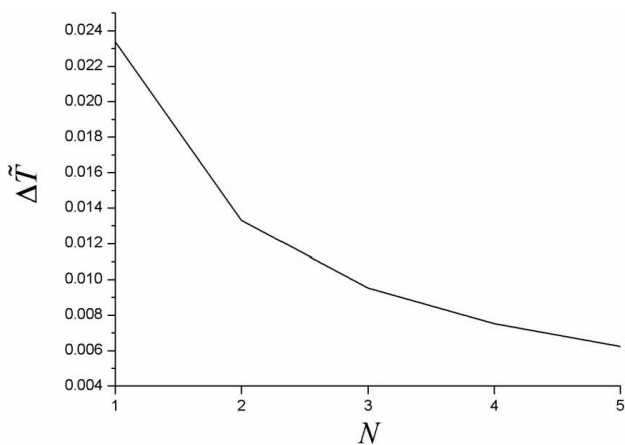


FIGURE 7. $\Delta\tilde{T}$ corresponding to $(\tilde{G}/\Delta\tilde{T})_{\max}$ versus N .

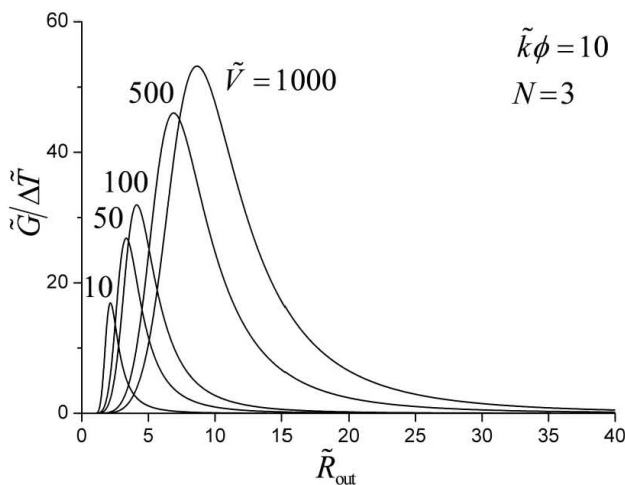


FIGURE 8. Effect of \tilde{V} on $\tilde{G}/\Delta\tilde{T}$ versus \tilde{R}_{out} with fixed $\tilde{k}\phi$ and N .

4.2. Maximization of $\tilde{G}/\Delta\tilde{T}$ at different \tilde{V}

$\tilde{G}/\Delta\tilde{T}$ versus \tilde{R}_{out} at a different \tilde{V} is shown in Fig. 8. There exists an $\tilde{R}_{out,opt}$ that $\tilde{G}/\Delta\tilde{T}$ achieves its maximum

and the performance of the electromagnet achieves its best. The bigger \tilde{V} is, the bigger $(\tilde{G}/\Delta\tilde{T})_{\max}$ is, and the better the performance of the electromagnet is. Fig. 9 shows that $(\tilde{G}/\Delta\tilde{T})_{\max}$ increases and then approaches a constant value as \tilde{V} increases. The corresponding $\tilde{R}_{out,opt}$ and \tilde{L}_{opt} versus \tilde{V} are shown in Fig. 10.

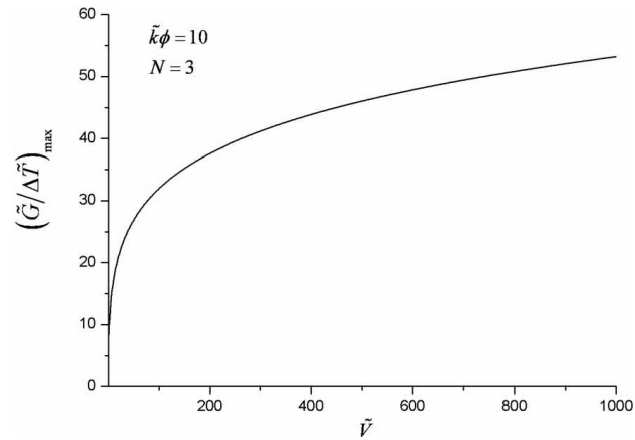


FIGURE 9. $(\tilde{G}/\Delta\tilde{T})_{\max}$ versus \tilde{V} with fixed $\tilde{k}\phi$ and N .

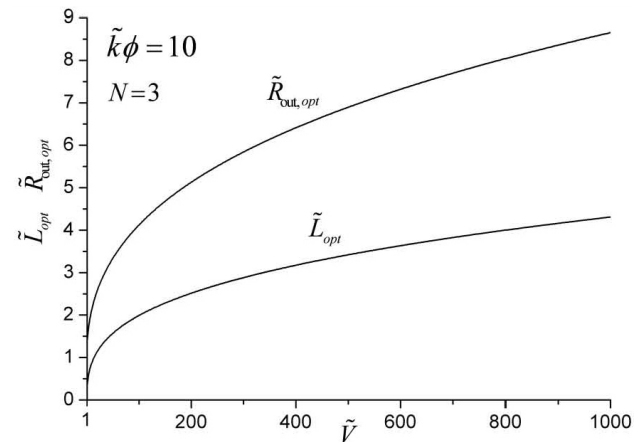


FIGURE 10. Optimal geometries $(\tilde{L}_{opt}, \tilde{R}_{out,opt})$ corresponding to $(\tilde{G}/\Delta\tilde{T})_{\max}$ versus \tilde{V} .

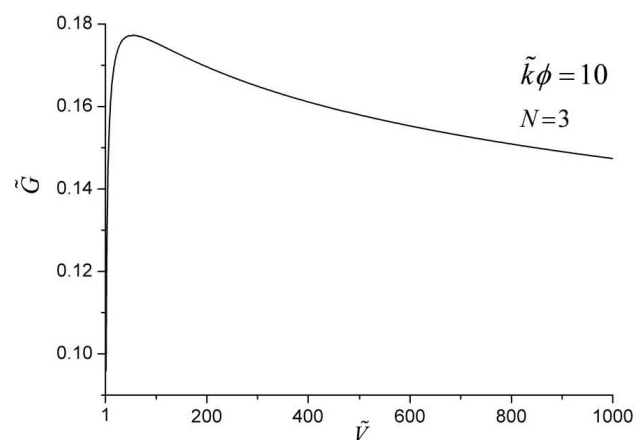


FIGURE 11. \tilde{G} corresponding to $(\tilde{G}/\Delta\tilde{T})_{\max}$ versus \tilde{V} .

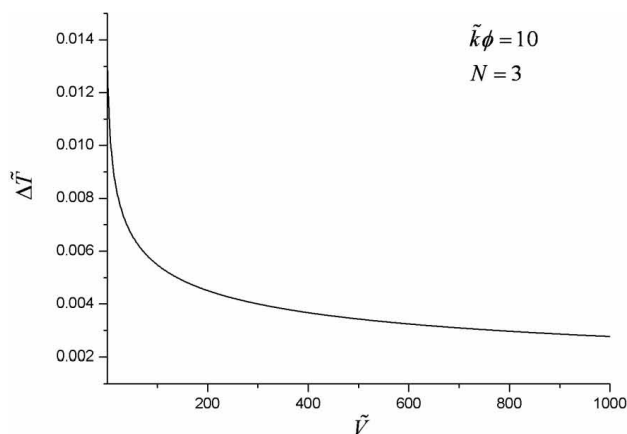


FIGURE 12. $\Delta\tilde{T}$ corresponding to $(\tilde{G}/\Delta\tilde{T})_{\max}$ versus \tilde{V} [33].

When the performance of the electromagnet achieves its best, the corresponding \tilde{G} versus \tilde{V} and $\Delta\tilde{T}$ versus \tilde{V} characteristics are shown in Fig. 11 and Fig. 12, respectively. As \tilde{V} increases, the magnetic induction \tilde{G} first increases and then decreases. The maximum temperature difference $\Delta\tilde{T}$ decreases as \tilde{V} increases.

5. Conclusion

Considering that the performance of the electromagnet requires a low maximum temperature difference and high mag-

netic induction, a complex-objective function $(\tilde{G}/\Delta\tilde{T})$ combining magnetic induction with maximum temperature difference is set up using the maximum temperature difference expression and magnetic induction expression deduced in Ref. 33. The new complex-objective function overcomes the disadvantage in Ref. 33 that the magnetic induction should be fixed as a constant when optimizing the electromagnet configuration. The optimization results show that the performance of the electromagnet is improved as the number of high thermal conductivity cooling discs inserted N increases. When $\tilde{G}/\Delta\tilde{T}$ achieves its maximum, the solenoid becomes longer and thinner as N increases. As N increases, the magnetic induction \tilde{G} increases and the maximum temperature difference $\Delta\tilde{T}$ decreases. $(\tilde{G}/\Delta\tilde{T})_{\max}$ also increases as \tilde{V} increases, and simultaneously, the magnetic induction \tilde{G} first increases and then decreases, and the maximum temperature difference $\Delta\tilde{T}$ decreases.

Acknowledgements

This paper is supported by The National Natural Science Foundation of P. R. China (Project No. 10905093), The Program for New Century Excellent Talents in University of P. R. China and The Foundation for the Author of National Excellent Doctoral Dissertation of P. R. China (Project No. 200136).

1. A. Bejan, *Shape and Structure, from Engineering to Nature* (Cambridge: Cambridge University Press, 2000).
2. A. Bejan and S. Lorente, *J. Non-Equilib. Thermodyn.* **26** (2001) 305.
3. R.N. Rosa, A.H. Reis, and A.F. Miguel, *Proceedings of the Symposium Bejan's Constructal Theory of Shape and Structure* (Evora: University of Evora, Portugal, 2004).
4. A. Bejan and S. Lorente, *The Constructal Law (La Loi Constructale)* (Paris: L'Harmattan, 2005).
5. A. Bejan and S. Lorente, *J. Appl. Phys.* **100** (2006) 041301.
6. A.H. Reis, *Appl. Mech. Rev.* **59** (2006) 269.
7. A. Bejan and J.H. Marden, *Am. Sci.*, **94** (2006) 342.
8. A. Bejan and G.W. Merckx, *Constructal Theory of Social Dynamics* (New York: Springer; 2007).
9. A. Bejan and S. Lorente, *Design with Constructal Theory*. (New Jersey: Wiley, 2008).
10. A. Bejan, S. Lorente, and A.F. Miguel, *Constructal Human Dynamics* (Security & Sustainability. Amsterdam: IOS Press, 2009).
11. S. Lorente, *Int. J. Energy Res.*, **33** (2009) 211.
12. A. Bejan and J.H. Marden, *Phys. Life Rev.* **6** (2009) 85.
13. A. Bejan, *J. Heat Transfer* **40** (1997) 799.
14. L. Gosselin, A. Bejan, and S. Lorente, *Int. J. Heat Mass Transfer* **47** (2004) 3477.
15. A.K. da Silva and L. Gosselin, *Int. J. Heat Mass Transfer*, **48** (2005) 609.
16. L.A.O. Rocha, S. Lorente, and A. Bejan, *Int. J. Heat Mass Transfer* **49** (2006) 2626.
17. S. Zhou, L. Chen, and F. Sun, *J. Phys. D: Appl. Phys.* **40** (2007) 3545.
18. W. Wu, L. Chen, and F. Sun, *Energy Convers. Manage.* **48** (2007) 101.
19. S. Zhou, L. Chen, and F. Sun, *Appl. Energy* **84** (2007) 505.
20. W. Wu, L. Chen, and F. Sun, *Appl. Energy* **84** (2007) 39.
21. S. Zhou, L. Chen, F. Sun, *Energy Convers. Mgmt.* **48** (2007) 106.
22. M. Joucaviel, L. Gosselin, and T. Bello-Ochende, *Int. Comm. Heat Mass Transfer* **35** (2008) 557.
23. L. Chen, S. Wei, and F. Sun, *J. Phys. D: Appl. Phys.* (2008) **41** 195506.
24. V.A.P. Raja, T. Basak, and S.K. Das, *Int. J. Heat Mass Transfer* **51** (2008) 3582.
25. L. Luo, Z. Fan, and H.L. Gall, *Chem. Engng. Proc.: Process Intensification* (2008) **47** 229.
26. G. Lorenzini and L.A.O. Rocha, *Int. J. Heat Mass Transfer* **52** (2009) 4683.

27. S. Wei, L. Chen, and F. Sun, *Appl. Energy* **86** (2009) 1111.
28. J. Dirker and J.P. Meyer, *Int. J. Heat Mass Transfer* **52** (2009) 1374.
29. P. Xu *et al.*, *Int. J. Therm. Sci.* **48** (2009) 2139.
30. K.M. Wang, S. Lorente, and A. Bejan, *Int. J. Heat Mass Transfer* (2009) **52** 4175.
31. A. Husain and K.Y. Kim, *Int. J. Heat Mass Transfer* (2009) **52** 5271.
32. H. Zhang, S. Lorente, and A. Bejan, *Int. J. Heat Mass Transfer* **52** (2009) 4327.
33. L. Gosselin and A. Bejan, *Int. J. Thermal Science*, **43** (2004) 331.
34. L. Chen, S. Wei, and F. Sun, *J. Appl. Phys.* **105** (2009) 094906.
35. Z. Guo, H. Zhu, and X. Liang, *Int. J. Heat Mass Transfer* **50** (2007) 2545.